Sustainable and Resilient Infrastructure

ISSN: 2378-9689 (Print) 2378-9697 (Online) Journal homepage: http://www.tandfonline.com/loi/tsri20

Efficiency index for fiber-reinforced concrete lining at ultimate limit state

Alessandro P. Fantilli, Kamran M. Nemati & Bernardino Chiaia

To cite this article: Alessandro P. Fantilli, Kamran M. Nemati & Bernardino Chiaia (2016) Efficiency index for fiber-reinforced concrete lining at ultimate limit state, Sustainable and Resilient Infrastructure, 1:1-2, 84-91, DOI: 10.1080/23789689.2016.1178558

To link to this article: https://doi.org/10.1080/23789689.2016.1178558

SUSTAINABLE AND RESILIENT INFRASTRUCTURE, 2016
VOL. 1, NOS. 1–2, 84–91
http://dx.doi.org/10.1080/23789689.2016.1178558

Taylor & Francis
Taylor & Francis Group

Efficiency index for fiber-reinforced concrete lining at ultimate limit state

Alessandro P. Fantilli[a], Kamran M. Nemati[b] and Bernardino Chiaia[a]

[a]Department of Structural, Building and Geotechnical Engineering, Politecnico di Torino, Torino, Italy; [b]Departments of Construction Management & Civil and Environmental Engineering, University of Washington, Seattle, WA, USA

ABSTRACT
The fiber contribution to the ultimate limit state capacity of precast and cast-*in situ* tunnel linings is analytically investigated. By means of a numerical model, capable of computing the interaction curves of reinforced concrete cross sections subjected to combined compressive and bending actions, the mechanical performances of plain and fiber-reinforced concrete are compared. As a result, a new index is introduced to quantify the effectiveness of fiber addition. The higher the efficiency index, the higher the amount of steel reinforcing bar that can be removed from a plain concrete cross section. The application to real concrete linings, where shear resistance is ensured without shear reinforcement, shows that a large volume of rebar can be saved by the presence of steel fibers. This gives significant advantages in terms of durability and rapidity of tunnel construction.

ARTICLE HISTORY
Received 16 December 2015
Accepted 4 April 2016

KEYWORDS
Fiber-reinforced concrete; efficiency index; ultimate limit state; cast-*in situ* concrete lining; precast tunnel segments

1. Introduction

Although the ITA-WG2 (International Tunnelling Association-Working Group 2) design guidelines are based on the use of traditional plain concrete (ITA-WG2, 2000), whose post-cracking tensile strength is neglected, several kinds of linings are made with fiber-reinforced concrete (FRC). Chiaia, Fantilli, and Vallini (2009b), for instance, described the design procedure of two cast-*in situ* tunnels in Italy, in which concrete lining is reinforced with both traditional steel bars and steel fibers. However, the most relevant application of FRC concerns precast tunnel segments (Vandewalle, 2005). Some of them have been built recently and are well described in the current literature. This is the case of the 3.9-km-long district heating tunnel in Copenhagen (Kasper, Edvardsen, Wittneben, & Neumann, 2008), of the 7.8-km-long Monte Lirio tunnel in Panama (Meda, Nerilli, & Rinaldi, 2012), and of the Line 9 subway of Barcelona (de la Fuente, Pujadas, Blanco, & Aguado, 2012).

The numerous advantages that FRC provides, both in precast and cast-*in situ* applications, justify the wide use of FRC lining. Concrete contains flaws and microcracks both in the material and interfaces even before an external load is applied. These defects and microcracks originate from excess water, bleeding, plastic settlement, thermal and shrinkage strains, and stress concentrations imposed by external restraints. Under applied loads, microcracks propagate, coalesce and form macrocracks (Nemati, 1997; Nemati, Monteiro, & Scrivener, 1998). The micro- and macro-fracturing processes can be vastly improved by adding randomly distributed fibers in concrete.

At ultimate limit state, the presence of steel fibers reduces the minimum reinforcement ratio of structural elements under bending moment and axial loads. As a result, lighter pre-curved and self-sustaining steel meshes can be used in these structures (Chiaia, Fantilli, & Vallini, 2007). Also the shear strength of concrete tunnels, which has to be ensured without using traditional reinforcement (i.e. stirrups), can be improved by the presence of steel fibers (Minelli & Plizzari, 2010).

In the serviceability limit stage, crack width detected in FRC structures is narrower than in plain concrete beams (Chiaia, Fantilli, & Vallini, 2009a). As the control of crack width is necessary to avoid the corrosion of steel rebar, and the premature failure of the structure, some durability requirements can be satisfied without increasing the amount of steel reinforcing bar (ACI 318, 1995; Eurocode 2, 2005). This is particularly true for precast tunnel segments, in which temporary loads (due to demolding, stacking, transportation, etc.), and the jack forces exerted by the boring machine, have to be taken into account (Plizzari & Tiberti, 2006).

CONTACT Kamran M. Nemati nemati@uw.edu

Finally, the use of fibers makes concrete structures more sustainable, especially when steel fibers are combined with mineral additives, such as fly ash and silica fume (Fantilli & Chiaia, 2013). Indeed, fibers not only suppress the formation of cracks, but also considerably reduce their propagation and growth, making concrete more ductile and durable, and therefore a more sustainable and resilient construction material. Resilience and sustainability are complementary and should be used in an integrated perspective. Resilience is an important attribute of sustainability, as it enhances the flexibility and adaptability of the system and increases the long-term benefits of a more durable material.

Nevertheless, the advantages of using FRC are not always guaranteed, neither exist models which quantify all the benefic effects of fibers, especially in tunnel linings (Caratelli, Meda, Rinaldi, & Romualdi, 2011). In the opinion of the authors, the efficiency index, introduced and applied for the first time in the present paper, is a useful tool to assess fiber reinforcement. By means of this index, the structural contribution provided by the presence of steel fibers is analytically evaluated in concrete cross section subjected to bending moment and compressive load. Accordingly, more sustainable and resilient concrete linings, containing a reduced amount of rebar, can definitely be designed by increasing the efficiency index of FRC.

2. The ultimate limit state of concrete linings

According to ITA-WG2 guidelines (ITA-WG2, 2000), the limit state design of concrete linings (Figure 1(a)) is schematically illustrated by the step-by-step procedure depicted in Figure 2. In step no. 1, the geometrical properties of the lining, and in particular, the thickness H of the lining cross section (Figure 1(b)), are introduced. Conversely, the mechanical response of structural materials, such as concrete strength class, steel type and, eventually, the type and the amount of fiber reinforcement, is defined in step no. 5. In the subsequent steps no. 6 and 7, the design values of the applied actions (bending moment – M_{Ed}, shear force – V_{Ed}, and axial force – N_{Ed}), related to the width B of the lining cross section (Figure 1(b)), are computed by means of analytical or numerical models.

In step no. 8, the values of M_{Ed}, V_{Ed}, and N_{Ed} are compared with the corresponding design strength values of the cross sections (i.e. M_{Rd}, N_{Rd}, V_{Rd}). To be more precise, the shear capacity of the cross section is firstly checked. If the condition $V_{Rd} \geq V_{Ed}$ is not satisfied in absence of shear reinforcement, the design procedure should restart at step no. 1 with a higher value of H, or at step no. 5 with a higher concrete strength class (Figure 2). When plain concrete or FRC lining fulfills the requirement $V_{Rd} \geq V_{Ed}$, then the cross-sectional areas A_{s1} and A_{s2} of the steel reinforcing bars need to be evaluated (Figure 1(b)). In accordance with Collins and Mitchell (2002), this can be done by computing the 'feasible region' (depicted in Figure 1(c)) of possible combinations of bending moment and axial loads. The boundary of this region is generally called the 'failure envelope' or 'interaction curve N_{Rd}–M_{Rd}'. As the values of N_{Ed} and M_{Ed} that lie outside the failure envelope cannot be sustained by the cross section, a suitable amount

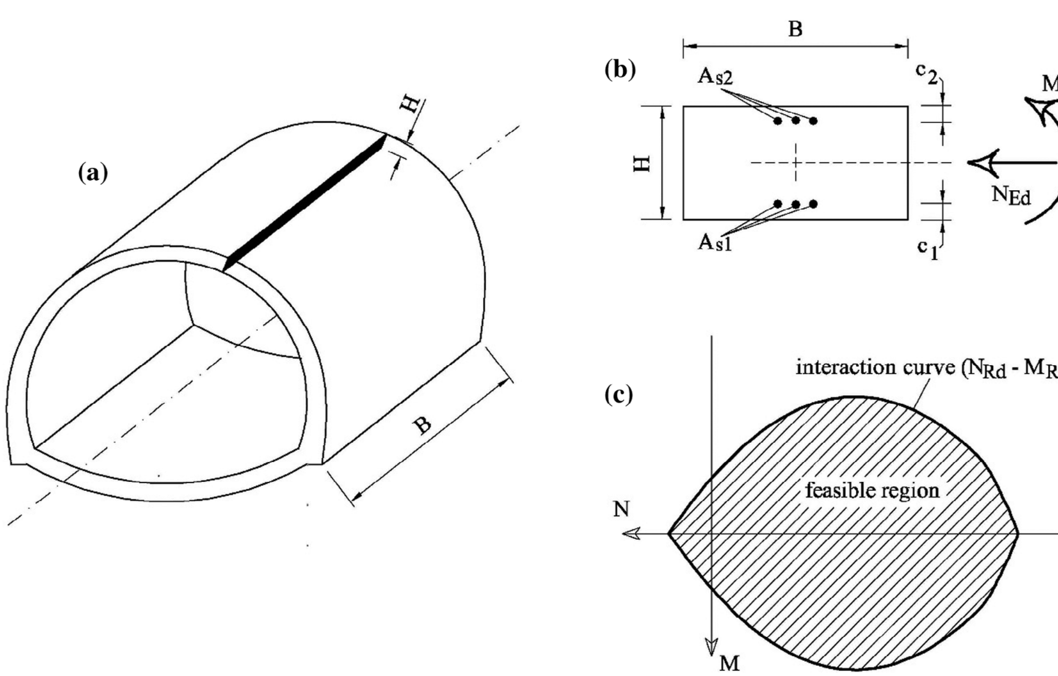

Figure 1. The ultimate limit state of concrete lining: (a) geometry of the tunnel; (b) longitudinal cross section; (c) interaction diagram of the cross section, which defines the feasibility region bordered by the curve N_{Rd}–M_{Rd}.
Notes: If the effects of the actions applied to the lining, i.e. N_{Ed}–M_{Ed}, fall within the feasibility region, the cross section can bear the applied loads.

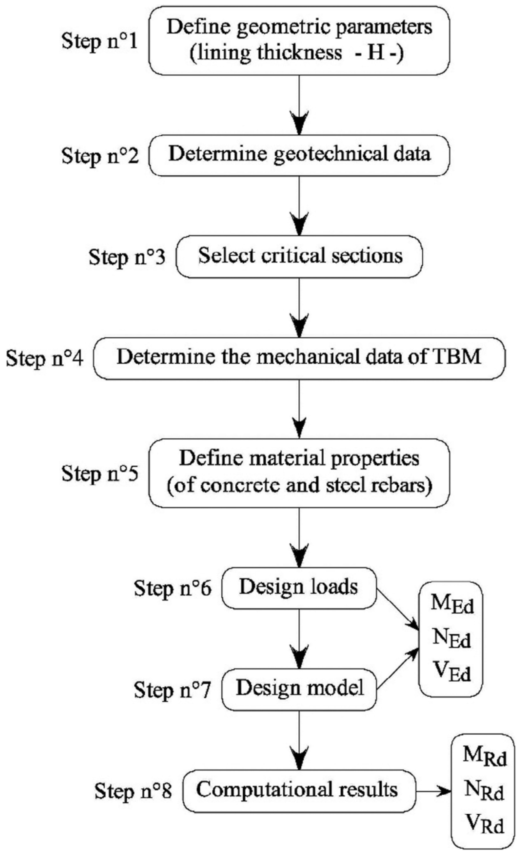

Figure 2. The steps of the design procedure suggested by ITA-WG2 (2000).

of A_{s1} and A_{s2} must be provided in order to contain all the applied actions within the interaction curve.

When the feasible region is computed, it is useful to evaluate the convenience of adding steel fibers to concrete, and to substitute completely, or partially, ordinary reinforcing bar. A new index, quantifying the fiber-reinforcement efficiency, is therefore introduced in the following sections.

3. The efficiency index of FRC

Traditionally, design of reinforced concrete cross sections under bending and axial loads is performed using so-called design charts (Park & Paulay, 1975). In these diagrams, the following dimensionless parameters are taken into consideration (see Figure 3):

$$\nu_{\mathrm{Rd}} = \frac{N_{\mathrm{Rd}}}{BHf_{\mathrm{cd}}} \tag{1a}$$

$$\mu_{\mathrm{Rd}} = \frac{M_{\mathrm{Rd}}}{BH^2 f_{\mathrm{cd}}} \tag{1b}$$

$$\omega = \frac{A_s f_{\mathrm{yd}}}{BHf_{\mathrm{cd}}} \tag{1c}$$

where ν_{Rd} = dimensionless axial load; μ_{Rd} = dimensionless bending moment; ω = mechanical reinforcement ratio; f_{cd}=design value of concrete compressive strength; f_{yd}= design yielding stress of steel reinforcing bars; and $A_s = A_{s1} + A_{s2}$ = global area of steel reinforcing bars.

Two groups of design charts are reported in Figure 3. All the ν_{Rd}–μ_{Rd} curves are related to the cross section drawn in

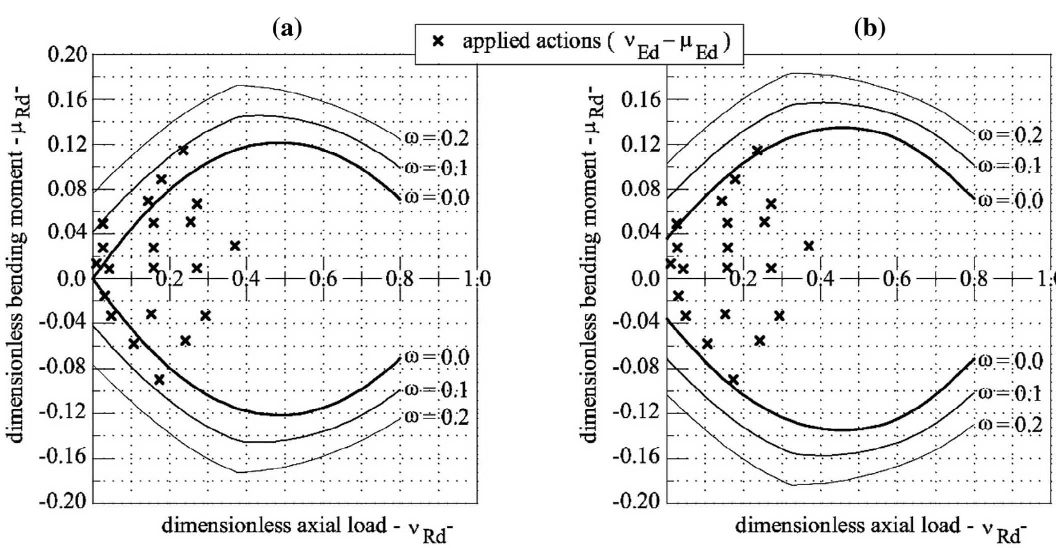

Figure 3. Interaction curves, in terms of dimensionless axial load ν_{Rd} *vs.* dimensionless bending moment μ_{Rd}, and applied actions: (a) design charts for plain concrete obtained for three dimensionless reinforcement ratios (ω = 0, .1, and .2); (b) design charts for FRC (ω = 0, .1, and .2). For the same values of ω and ν_{Rd}, the bending capacity of the FRC cross section (i.e. μ_{Rd}) is generally higher than that of plain concrete.

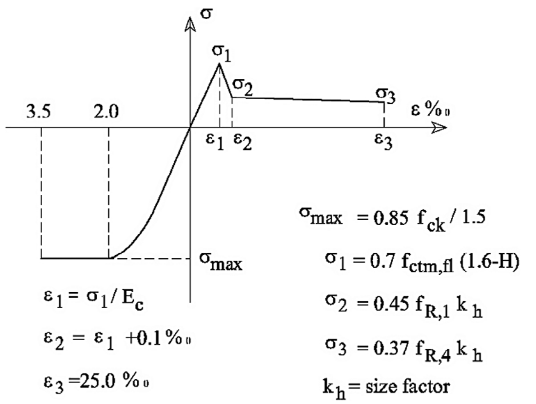

Figure 4. The stress–strain relationship of concrete.
Notes: Post-cracking tensile stresses exist only in presence of fibers, when $f_{R,1}$ and $f_{R,4}$ are higher than zero (Rilem TC 162 – TDF, 2003).

Figure 1(b) ($c_1/H = c_2/H = .2$, $A_{s1} = A_{s2}$), in which C40/50 is the concrete strength class, and B450C is the type of steel rebar. The design chart in Figure 3(a), composed by three interaction curves, is here computed in the case of plain concrete by assuming the parabola–rectangle stress–strain relationship for compressed concrete (Eurocode 2, 2005) and neglecting the contribution of concrete in tension (i.e. $\sigma_1 = \sigma_2 = \sigma_3 = 0$ in Figure 4). The complete numerical procedure used to obtain these design charts is described by Chiaia et al. (2007). An interaction curve is obtained in absence of reinforcement ($\omega = .0$), whereas the other curves are related to two ordinary amount of rebar ($\omega = .1$ and .2). Due to the symmetry of concrete cover and of steel reinforcement areas, the interaction curves show symmetry with respect to the horizontal axis (or the dimensionless axial load, assumed to be positive in compression). In addition, when $\nu_{Rd} = 0$, the cross section cannot resist the bending moment without flexural reinforcement (i.e. $\mu_{Rd} = 0$ when $\omega = 0$).

If steel fibers are introduced in the concrete cast, tensile stresses also persist in the case of large crack width (or high tensile strains). As a consequence, interaction domains show a bending capacity in absence of rebar and axial loads (i.e. $\mu_{Rd} \neq 0$, when $\omega = 0$ and $\nu_{Rd} = 0$). This is clearly evident in the design charts depicted in Figure 3(b), concerning a rectangular cross section made with the same type of reinforcing bars (B450C) and concrete (C40/50), but with 40 kg/m^3 of steel fibers having hooked ends (length 30 mm, diameter .35 mm), as used by Caratelli et al. (2011). Those reported in Figure 3(b) are only some of the possible design charts, which can be obtained by adding fibers to a cementitious matrix. Indeed, μ_{Rd}–ν_{Rd} feasibility regions are a function of σ_2 and σ_3 (Figure 4), which in turn depend on the content, the aspect ratio, and the shape (straight or with hooked ends) of the fibers. As the latter relationship cannot be defined with simply theoretical models, tests are necessary to define the stresses σ_2 and σ_3 for a pre-established FRC. In particular, Rilem TC 162 – TDF (2003) suggests testing FRC beams in three-point bending, measuring the so-called residual strengths $f_{R,1}$ and $f_{R,4}$, and calculating σ_2 and σ_3 with the formulae reported in Figure 4.

In both the design charts in Figure 3, the applied bending moment and axial loads are reported. In the case of plain concrete (Figure 3(a)), the couples ν_{Ed}–μ_{Ed} fall within the feasibility region limited by the interaction curve with $\omega = .1$. The amount of rebar can be reduced in the case of FRC (Figure 3(b)), even if the ordinary steel reinforcing bars cannot be eliminated. Indeed, the interaction curve of FRC with $\omega = 0$ does not contain all the applied actions (see Figure 3(b)).

From a design point of view, it is interesting to quantify the reduction of ω due to the presence of fiber reinforcement. Obviously, the higher the efficiency of the fibers, the lower the amount of rebar necessary for the section to bear the same applied loads. Thus, the introduction of an efficiency index of FRC can be useful to reduce, and sometimes even eliminate, the amount of steel reinforcing bar. A possible definition of this index is illustrated in Figure 5(a), where the interaction curve of plain concrete (Curve 1) and that of FRC (Curve 2), both evaluated when $\omega = .1$, are reported. In the same Figure, Curve 3 borders the feasibility region of the FRC computed in the case of $\omega = .1\,(1 - I_{FRC})$, where I_{FRC} is the efficiency index of the FRC:

$$I_{FRC} = \frac{\mu_2 - \mu_1}{\mu_1} \tag{2}$$

where μ_1 = dimensionless bending moment of Curve 1 when $\nu_{Rd} = 0$; μ_2 = dimensionless bending moment of Curve 2 when $\nu_{Rd} = 0$.

As Figure 5(a) shows, Curve 3 matches Curve 1 in the case of low dimensionless axial loads, whereas it becomes more conservative when $\nu_{Rd} > .3$. As all the couples ν_{Ed}–μ_{Ed} fall within the feasible region bordered by Curve 3, the proposed I_{FRC} can be effectively used to evaluate both the efficiency of fiber reinforcement, and the reduction of rebar used in a plain concrete cross section.

It must be remarked that the efficiency index can vary. For the same cross section and materials, I_{FRC} depends on the amount of rebar necessary to obtain, in a plain concrete solution, a feasible region capable of containing all the applied actions. As illustrated in Figure 5(b), the efficiency index decreases with ω, as already observed in the numerical and experimental parametric study of Taheri, Barros, and Salehian (2012). Hence, in presence of highly reinforced concrete structures, the introduction of a fiber reinforcement does not give significant advantages, in terms of saving ordinary reinforcing bar. This is

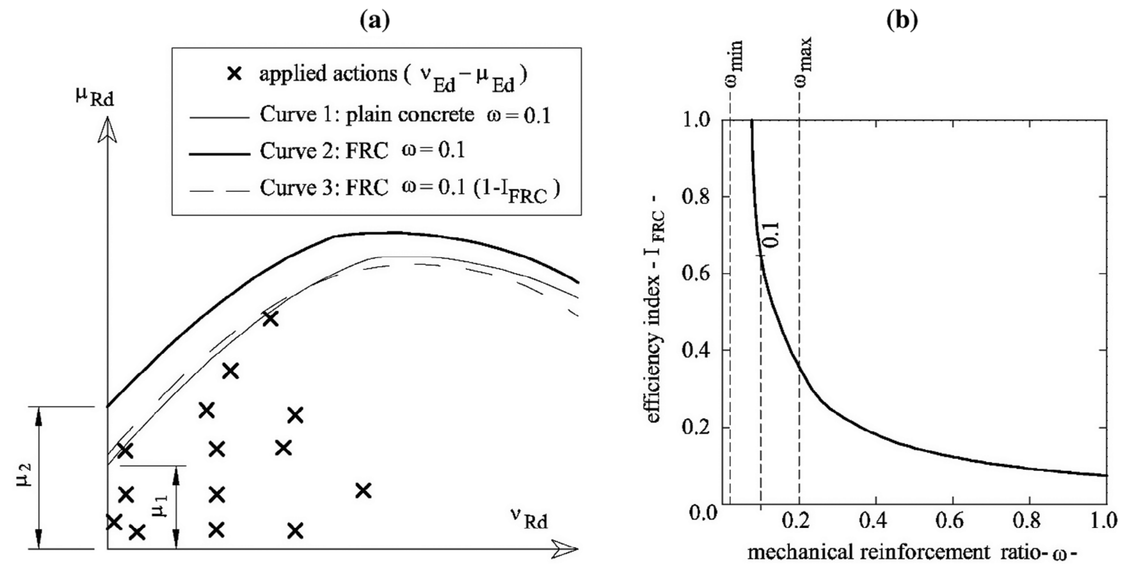

Figure 5. Definition and use of I_{FRC}: (a) the design charts for plain reinforced concrete (Curve 1 with $\omega = .1$) and two FRCs (Curve 2 with $\omega = .1$, and Curve 3 with $\omega = .1\ (1 - I_{FRC})$); (b) fiber-reinforcement efficiency as a function of the dimensionless reinforcement ratio ω.
Notes: The reference value $\omega = .1$ is between the maximum and minimum values suggested by building codes.

due to the low residual tensile strength provided by FRC. In fact, bridging stresses on the crack surfaces are lower than the tensile strength, which in turn is nearly 10 times lower than the compressive strength of an ordinary concrete or FRC. For these reasons, only in lightly reinforced concrete structures, such as the massive dimensions of the cross sections of tunnel linings subjected to ν_{Ed}–μ_{Ed}, can the tensile contribution of FRC be comparable to that of rebar. Thus, in the present case, steel reinforcing bars can be effectively substituted by, or used in combination with, steel fiber when $\omega < .4$ ($I_{FRC} > .2$ in Figure 5(b)).

A minimum reinforcement ratio ω_{min} should always be exceeded by ω, in order to prevent brittle failure of RC cross section (Park & Paulay, 1975). The value $\omega_{min} = .02$ reported in Figure 5(b) can be computed by means of the nonlinear model proposed by Chiaia et al. (2007). Conversely, to avoid crushing of compressive concrete before the yielding of rebar in tension, the maximum reinforcement ratio $\omega_{max} = .2$ cannot be exceeded (Park & Paulay, 1975). In the present case, $\omega = .1$ is between the upper and the lower bounds of the mechanical reinforcement ratio, and, consequently, the value $I_{FRC} = .6$ can be accepted (Figure 5(b)). Nevertheless, when I_{FRC} is higher than 1 (or $\mu_2/\mu_1 > 2$), all the rebar can be substituted by the fibers. In fact, in this case, the non-dimensional reinforcement ratio of Curve 3 (Figure 5(a)) is negative (i.e. $I_{FRC} - 1 < 0$). However, a certain reduction of the fiber volume fraction could be more appropriate in many practical situations, rather than the complete substitution of rebar with a large amount of fibers.

4. Some applications

The efficiency index I_{FRC} quantifies the structural advantages provided by steel fibers, as well as the reduction of ordinary rebar used to reinforce concrete linings. Such an index has been adopted in the feasibility design analyses of several tunnels. In the following sections, two applications are respectively described for cast-*in situ* and precast concrete linings.

4.1. The Shaanxi tunnel

The Shaanxi tunnel is a water-diversion tunnel from Hanjiang River to Wei River in the Shaanxi province of China. The geometrical dimensions of the cross section, computed in accordance with the design procedure illustrated in Figure 2, are reported in Figure 6. The thickness H = 450 mm is sufficient to satisfy the condition $V_{Rd} \geq V_{Ed}$ without any shear reinforcement in both plain concrete and FRC lining. Using I_{FRC}, it is possible to quantify the advantage of replacing the final lining of the tunnel, expected to be made by ordinary concrete and steel rebar (called Plain concrete-solution), with steel fiber-reinforced concrete and rebar (called FRC-solution). The mechanical properties of the materials used in both the solutions are reported in Figure 6. In all the cases, C30/37 concrete strength and steel reinforcing bar having a characteristic yielding strength f_{yk} = 335 MPa are used. In the FRC solution, 30 kg of Dramix RC-80/60-BN steel fibers are added to a cubic meter of concrete. Figure 6 also shows the values of the residual tensile strengths, experimentally

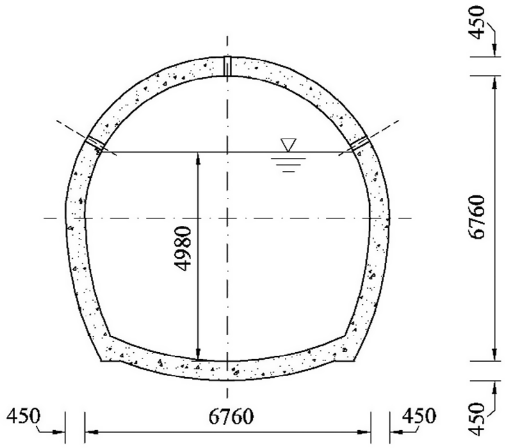

	Plain concrete Solution	FRC Solution
f_{ck}	30 MPa	30 MPa
$f_{ctm,fl}$	–	4.8 MPa
$f_{R,1}$	–	3.8 MPa
$f_{R,4}$	–	3.3 MPa
k_h	–	0.5
f_{yk}	335 MPa	335 MPa

Figure 6. Geometrical and mechanical properties of the Shaanxi tunnel (China).

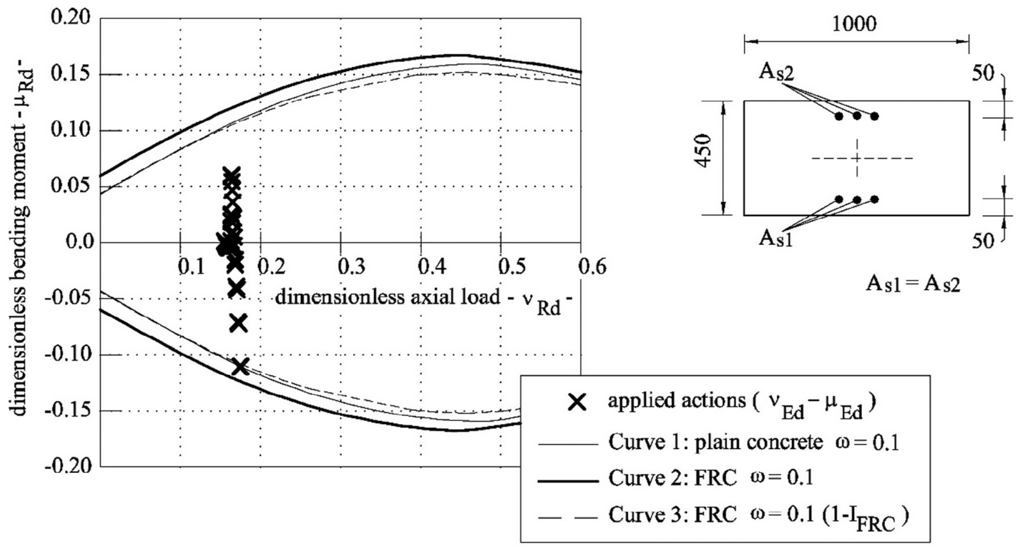

Figure 7. Three design charts for the cross section of the Shaanxi tunnel (China), concerning the cases of plain concrete (Curve 1 with $\omega = .1$) and two FRCs (Curve 2 with $\omega = .1$, and Curve 3 with $\omega = .1\ (1 - I_{FRC})$).

evaluated by testing FRC beams in three-point bending (Rilem TC 162 – TDF, 2003).

The calculated ν_{Ed}–μ_{Ed} actions, defined in each cross section of the lining, are reported in the interaction diagram of Figure 7. All these couples are bordered by the interaction curve of the plain concrete cross section reinforced with $\omega = .1$ (Curve 1 in Figure 7). The comparison between Curve 1 and Curve 2 (i.e. the interaction curve of the FRC solution at the same reinforcement ratio – Figure 7) reveals that the combination of steel fibers and rebar reduces the value of ω. Indeed, Equation (2) gives $I_{FRC} = .4$, and therefore 30 kg/m^3 of fibers and a mechanical reinforcement ratio $\omega = .1\ (1 - I_{FRC}) = .06$ are sufficient to define a feasible region that contains all the applied actions (Curve 3 in Figure 7).

As the minimum reinforcement ratio is equal to $\omega_{min} = .05$ (Chiaia et al., 2007), the proposed FRC solution also satisfies the condition $\omega_{min} \le \omega \le \omega_{max.}$

4.2. The Coca Codo Sinclair tunnel

This is a precast tunnel (25 km in length) designed for the hydro-electric project called Coca Codo Sinclair (Ecuador). Figure 8 shows the geometrical dimensions of the tunnel segment, as well as the mechanical properties of the materials adopted, respectively, in the plain concrete solution (concrete strength C40/50) and the FRC solution (40 kg of Dramix RC-80/60-BN steel fibers added to a cubic meter of C40/50 concrete). Residual tensile strengths have been measured by testing FRC beams

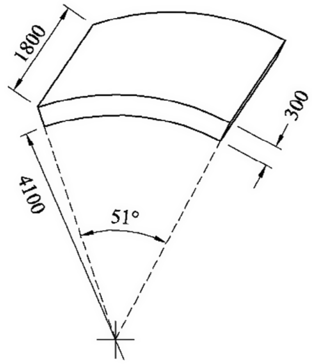

	Plain concrete Solution	FRC Solution
f_{ck}	40 MPa	40 MPa
$f_{ctm,fl}$	–	5.8 MPa
$f_{R,1}$	–	5.0 MPa
$f_{R,4}$	–	4.3 MPa
k_h	–	0.7
f_{yk}	450 MPa	450 MPa

Figure 8. Geometrical and mechanical properties of the Coca – Codo Sinclair tunnel (Ecuador).

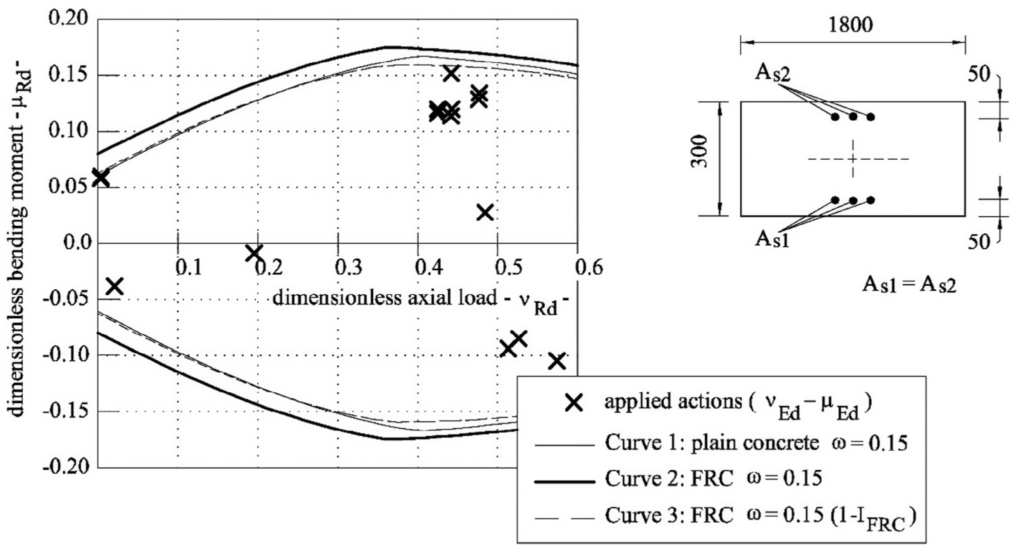

Figure 9. Three design charts for the cross section of the Coca Codo Sinclair tunnel (Ecuador), concerning the cases of plain concrete (Curve 1 with $\omega = .15$) and two FRCs (Curve 2 with $\omega = .15$, and Curve 3 with $\omega = .15\ (1 - I_{FRC})$).

in three-point bending, as suggested by Rilem TC 162 – TDF (2003).

As the height $H = 300$ mm has been computed by adopting the design procedure depicted in Figure 2 (ITA-WG2, 2000), the lining (Figure 9) does not need shear reinforcement to satisfy the inequality $V_{Rd} \geq V_{Ed}$. By means of the same procedure, the applied actions ν_{Ed}–μ_{Ed} have been also computed in each cross section of the lining, as reported in the design chart of Figure 9. If the characteristic strength of the rebar is $f_{yk} = 450$ MPa, $\omega = .15$ is sufficient to envelope all the applied loads in the plain concrete solution (Curve 1 in Figure 9). The same is also true for the FRC solution having the same mechanical reinforcement ratio (Curve 2 in Figure 9), even if the value of ω can be significantly reduced. As Equation (2) gives $I_{FRC} = .32$, the FRC solution, combined with $\omega = .15\ (1 - I_{FRC}) = .1$ (i.e. Curve 3 in Figure 9), satisfies the ultimate limit state requirement as well. Such an amount of steel rebars is higher than the minimum reinforcement ratio $\omega_{min} = .05$ (Chiaia et al., 2007), and therefore the proposed FRC solution also satisfies the condition $\omega_{min} \leq \omega \leq \omega_{max}$.

5. Conclusions

The numerical analyses developed in the present paper concerning the efficiency of fiber reinforcement in concrete lining lead to the following conclusions:

- The interaction curve of reinforced concrete cross sections, subjected to bending moments and axial loads, can be significantly modified by a low volume of steel fibers (less than 40 kg per cubic meter of concrete).
- At the ultimate limit state, the contribution, or the efficiency, of fiber reinforcement is higher in structures with massive dimension of the cross section subjected to low axial loads.

- The effectiveness of fiber additions can be quantitatively measured by the efficiency index I_{FRC} (Equation 2).
- The feasibility study of two reinforced concrete linings, whose cross sections can resist shear actions without shear reinforcement, shows that the performances of FRC are comparable with that of plain concrete having a higher amount of rebar.

The proposed index, here applied to the ultimate limit states, can be extended to the serviceability performances and, in the case of shield tunnel linings, to the capability of FRC to resist to the thrust pressure of a tunnel boring machine. In other words, all the beneficial effects of fiber reinforcement, including bursting resistance and higher sustainability, should be investigated in future works to determine a more general efficiency index.

Acknowledgments

The authors wish to express their gratitude to Bekaert SA for the technical suppsort.

Disclosure statement

No potential conflict of interest was reported by the authors.

Notes on contributors

Alessandro P. Fantilli is an associate professor in the Department of Structural, Building, and Geotechnical Engineering of Politecnico di Torino, Turin, Italy. He received his MS and PhD from Politecnico di Torino. He is a member of ACI committee 544 – Fiber-reinforced concrete – and 555 – Concrete with Recycled Materials His research interests include nonlinear analysis of reinforced concrete structures, and structural application of high-performance fiber-reinforced cementitious concrete.

Kamran M. Nemati, FASCE, FACI, is an associate professor in the Departments of Construction Management and Civil and Environmental Engineering at the University of Washington, Seattle, WA. He received his PhD in civil engineering from the University of California at Berkeley, Berkeley, CA. His research interests include fracture mechanics of concrete, microstructure, experimental methods leading to preservation of cracks in concrete under load, sustainability, and concrete pavements.

Bernardino Chiaia is a professor of Structural Mechanics in the Department of Structural, Building, and Geotechnical Engineering of Politecnico di Torino, Turin, Italy. He is the Vice-Rector of Politecnico di Torino in charge for Foreign Affairs. He received his PhD from Politecnico di Torino. His research interests include fracture mechanics and structural integrity, complex systems in civil engineering, and high-performance materials.

ORCID

Kamran M. Nemati http://orcid.org/0000-0002-4318-7931

References

ACI 318. (1995). *Building code requirements for structural concrete*. Farmington Hills, MI: American Concrete Institute.

Caratelli, A., Meda, A., Rinaldi, Z., & Romualdi, P. (2011). Structural behaviour of precast tunnel segments in fiber reinforced concrete. *Tunnelling and Underground Space Technology, 26*, 284–291.

Chiaia, B., Fantilli, A. P., & Vallini, P. (2007). Evaluation of minimum reinforcement ratio in FRC members and application to tunnel linings. *Materials and Structures, 40*, 593–604.

Chiaia, B., Fantilli, A. P., & Vallini, P. (2009a). Evaluation of crack width in FRC structures and application to tunnel linings. *Materials and Structures, 42*, 339–351.

Chiaia, B., Fantilli, A. P., & Vallini, P. (2009b). Combining fiber-reinforced concrete with traditional reinforcement in tunnel linings. *Engineering Structures, 31*, 1600–1606.

Collins, M. P., & Mitchell, D. (2002). *Prestressed concrete structures*. Englewood Cliffs: Prentice Hall.

de la Fuente, A., Pujadas, P., Blanco, A., & Aguado, A. (2012). Experiences in Barcelona with the use of fibres in segmental linings. *Tunnelling and Underground Space Technology, 27*, 60–71.

Eurocode 2. (2005). *Design of concrete structures - Part 1: General rules and rules for buildings*. ENV 1992-1-1. Brussels: European Committee for the Standardization.

Fantilli, A. P., & Chiaia, B. (2013). Eco-mechanical performances of cement-based materials: An application to self-consolidating concrete. *Construction and Building Materials, 40*, 189–196.

ITA-WG2. (2000). Guidelines for the design of shield tunnel lining. *Tunnelling and Underground Space Technology, 15*, 303–331.

Kasper, T., Edvardsen, C., Wittneben, G., & Neumann, D. (2008). Lining design for the district heating tunnel in Copenhagen with steel fibre reinforced concrete segments. *Tunnelling and Underground Space Technology, 23*, 574–587.

Meda A., Nerilli F., & Rinaldi Z. 2012. Numerical modeling of precast FRC segments: the Monte Lirio tunnel in Panama. In: *BEFIB2012 – 8th RILEM international symposium on fibre reinforced concrete*. Guimarães, Poutugal, September 19–21.

Minelli, F., & Plizzari, G. (2010). *Shear and punching shear in RC and FRC elements. fib Bulletin No. 57*. Lausanne: International Federation for Structural Concrete (fib).

Nemati, K. M. (1997). Fracture analysis of concrete using scanning electron microscopy. *Scanning, The Journal of Scanning Microscopies, 19*, 426–430.

Nemati, K. M., Monteiro, P. J. M., & Scrivener, K. L. (1998). Analysis of compressive stress-induced cracks in concrete. *American Concrete Institute Materials Journal, 95*, 617–631.

Park, R., & Paulay, T. (1975). *Reinforced concrete*. New York, NY: John Wiley and Sons. Inc.

Plizzari, G. A., & Tiberti, G. (2006). Steel fibers as reinforcement for precast tunnel segments. *Tunnelling and Underground Space Technology, 21*, 438–439.

Rilem TC 162 – TDF. (2003). σ– ε design method: Final recommendation. *Materials and Structures, 36*, 560–567.

Taheri, M., Barros, J. A. O., & Salehian, H. (2012). Parametric study of the use of strain softening/hardening FRC for RC elements failing in bending. *Journal of Materials in Civil Engineering, 24*, 259–274.

Vandewalle, M. (2005). *Tunneling is an art*. Zwevegem: NV Bekaert SA.